ISJ 19: 42-52, 2022 ISSN 1824-307X

RESEARCH REPORT

Characterization of a Novel C-type Lectin against OsHV-1 infection in *Scapharca broughtonii*

D Wang[1,2,3], B Huang[2,3], J Yu[2,3,4], C Bai[2,3], C Li[2,3], C Wang[2,3], L Xin[2,3*], H Zhou[1*]

[1]Hainan University, Haikou, 570228, PR China
[2]Function Laboratory for Marine Fisheries Science and Food Production Processes, Qingdao National Laboratory for Marine Science and Technology, Qingdao 266071, PR China
[3]Qingdao Key Laboratory of Mariculture Epidemiology and Biosecurity, Key Laboratory of Maricultural Organism Disease Control, Ministry of Agriculture, Yellow Sea Fisheries Research Institute, Chinese Academy of Fishery Sciences, Qingdao 266071, PR China
[4]Dalian Ocean University, Dalian 116023, PR China

 Accepted March 2, 2022

Abstract

As important pattern recognition receptors (PRRs), most C-type lectins (CTLs) are a class of Ca^{2+}-dependent carbohydrate-binding proteins that are found to be involved in non-self-recognition and antiviral process. In this study, a new CTL, named SbCTL, was identified from ark clams, *Scapharca broughtonii*. The amino acid sequence of SbCTL consisted of a predicted CRD (carbohydrate recognition domain) structural domain (including 102 amino acid residues). The amino acid sequence of SbCTL shared 28 % - 39 % similarity with other CTLs. There were two potential Ca^{2+} binding sites in SbCTL. The expression of SbCTL mRNA was detected in all selected tissues, with the highest expression in the gills. Expression of SbCTL mRNA increased significantly ($p < 0.05$) and total vibrio content increased significantly ($p < 0.05$) in ark clam infected with OsHV-1 at 72 h post-infection. The binding activities of recombinant SbCTL (rSbCTL) to various PAMPs with or without Ca^{2+} were analyzed by ELISA, rSbCTL showed especially high binding activity to LPS in a Ca^{2+}-independent manner. rSbCTL also functioned on sheltering ark clams from OsHV-1 infection *in vivo*, there were less mortality occurred in the rSbCTL treated group than the control. In all, it suggests that SbCTL, could served a critical role in the immune response against intruders in ark clams.

Key Words: *Scapharca broughtonii*; C-type lectin; PAMP binding; OsHV-1 infection

Introduction

Pattern recognition receptor-mediated recognition of pathogen-associate molecular patterns (PAMPs) is a key defense component in invertebrate innate immunity (Vasta *et al.*, 2004). As a family of pattern recognition receptors, C-type lectins (CTLs) could execute recognition and binding activity to a variety of carbohydrate ligands in immune defense which would regulate the expression of signaling molecules and inflammatory responses, further induce apoptosis or other immunological effect on pathogen killing and clearance (Shi *et al.*, 2004; Eisen, 2010). In red swamp crayfish, a CTL, PcLec6, was found to motivate crayfish defense system against pathogen invasion by initial recognition of pathogens and up-regulation of immune effectors such as anti-lipopolysaccharide factor (ALF) (Zhang *et al.*, 2018). In *Marsupenaeus japonicus*, two CTLs, LdlrLec1 and LdlrLec2, were found to protect shrimp from white spot syndrome virus (WSSV) infection by binding to WSSV vesicle protein VP28 and inhibiting viral replication (Qian *et al.*, 2012). Another CTL of *Penaeus vannamei* (LvCTLD) is involved in shrimps against the invasion of yellow head virus (YHV) by means of recruiting hemocytes to the site of virus infection and activating the prophenoloxidase cascade system (proPO system) (Junkunlo *et al.*, 2012).

CTLs commonly contain one or more carbohydrate recognition domains (CRDs). A single CRD consists of 110-130 amino acids, featured by internal and external bilayer structures. Its

Corresponding authors:
Lusheng Xin
Function Laboratory for Marine Fisheries Science and Food Production Processes
Qingdao National Laboratory for Marine Science and Technology
Qingdao 266071, PR China
E-mail: xinls@ysfri.ac.cn
Hailong Zhou
Hainan University
Haikou 570228, PR China
E-mail: zhouhl@hainu.edu.cn

three-dimensional structure is reinforced by two pairs of highly conserved disulphide bonds at the base layer (Zelensky and Gready, 2005). There are usually four Ca^{2+}-binding domains in each CRD. Ca^{2+} plays an important role in CRD structure maintaining the ligand binding activity. The carbohydrate binding sites of CRDs are diverse, such as EPN, QPD, QPE, EPG, NPR (Zhang *et al.*, 2009a; Qian *et al.*, 2012b). CRDs entitled CTLs the activities of recognition and binding to the polysaccharides of intruders (Zelensky and Gready, 2005; Luo *et al*., 2007).

CTLs with a single CRD have greater specificity, while those with multiple CRDs show broader recognition spectrum (Zhang, *et al*., 2009; Wang, *et al*., 2012). In oysters, CgCLec-3 containing a single CRD showed the strongest binding activity to PGN among tested PAMPs (Song *et al.*, 2019). In the silkworm *Bombyx mori*, a CTL named BmMBP, containing two CRDs, each one had dissimilar binding spectra to sugars. CRD1 bound to teichoic acid and mannan, CRD2 bound to teichoic acid, peptidoglycan, and mannan, PAMPs of Gram-positive bacteria and yeasts. These properties contribute to the multi-recognition characteristic of BmMBP (Watanabe *et al.*, 2006). In *Chlamys farreri*, a CTL named CfLec-4 with four CRDs showed strong binding activity to a variety of PAMPs including LPS, PGN, Mannan and Glucan, resulting in that CfLec-4 could bind to diverse microorganisms including Gram-negative bacteria, Gram-positive bacteria and yeasts (Wu *et al.*, 2012; Wang *et al.*, 2013).

Ark clam, *Scapharca broughtonii*, is a large marine benthic bivalve and mainly distributes in the offshore water of Northern Asia (Zhao *et al.*, 2018)，It is susceptible to ostreid herpesvirus-1 (OsHV-1) infection as oysters and other bivalves. Mass mortalities of ark clams and other culture bivalves are frequently occurred due to OsHV-1 infection (Ren *et al.*, 2013). Thus, much attention has been attracted on bivalve molecular immune mechanisms in order to achieve effective prevention and control of the OsHV-1 disease. Bivalve CTLs are multitudinous and conservatively execute initial non-self recognition. However, it is largely unknown how bivalve CTLs would function in response to OsHV-1 infection. In this study, a novel C-type lectin SbCTL was characterized from ark clam, *S. broughtonii*, with the aim of exploring the molecular functions of SbCTL, investigating its protective effects on ark clams against OsHV-1 *in vivo*. The results of this study will deep our understanding on the role of C-type lectins in bivalve innate immunity.

Materials and methods

Ark clams, experimental infection and sample collection

Ark clams were obtained from a local aquaculture farm in Qingdao, China and were acclimated in air-pumped seawater under temperature 16 ± 2 °C, DO 5 mg/L, salinity 30 ± 1 ‰, pH 7.5-8.5 for two weeks prior to the following experiments.

Different tissues, including hepatopancreas, hemocytes, gill, mantle, adductor muscle and foot, were dissected from six healthy ark clams as parallel samples to investigate the mRNA distribution of SbCTL.

For experimental infection, OsHV-1 inoculum was prepared as described by Schikorski (Sorvillo *et al.*, 2011) with modification. Briefly, the mantle tissues from OsHV-1 positive ark clams were split and homogenized. Then mantle homogenate was centrifuged at 1000 r/min for 15 min at 4 °C, the precipitate was discarded and the supernatant was filtered through a 0.22 μm pore size filter. Meanwhile, the mantle tissues from OsHV-1 negative ark clams were parallelly treated to prepare OsHV-1 negative inoculum for the control group.

A total of 100 ark clams were randomly selected for virus inoculation by injection with 100 μL prepared OsHV-1 inoculum (~10^5 copies of viral DNA/μL). Another 100 ark clams received an injection with the same volume of OsHV-1 negative inoculum as the control group. Nine individuals of each group were randomly sampled at 0, 6, 12, 24, 48 and 72 h post injection. Three hemocyte samples were prepared for each treatment by centrifugation of the mixed hemolymph of three random individuals.

RNA extraction and cDNA synthesis

Total mRNA was extracted from hemocytes using Trizol reagent (Invitrogen) according to the manufacture's protocol. The first-strand cDNA synthesis was carried out based on M-MLV RT Usage information using the DNase I (Promega) treated total mRNA as template and oligo (dT)-adaptor primer (Table 1). The reaction mixtures were incubated at 50 °C for 1 h, terminated by heating at 85 °C for 5 min. The cDNA mix was diluted to 1:20 and stored at -80 °C for subsequent quantitative Real-time PCR (qRT-PCR) analysis.

cDNA clone and sequence analyses of SbCTL *gene*

A highly homologous sequence to CTL was identified in the transcriptome data of *S. broughtonii*. Its complete open reading frame (ORF) was predicted by ORF finder in the National Center for Biotechnology Information (http://www.ncbi.nlm.nih.gov/). A pair of specific primers SbCTL-F and SbCTL-R (Table 1) were designed to clone the ORF sequence of SbCTL using Primer 5 according to the sequence information of the transcriptome assembly results. PCR products were gel-purified and verified by sequencing.

The Expert Protein Analysis System (http://www.expasy.org/) was used to deduced the amino acid sequence of SbCTL. The conserved protein domain of SbCTL was revealed by the simple modular architecture research tool (SMART) version 4.0 (http://www.smart.emblheidelberg.de/). The presumed tertiary structure of SbCTL was established using Iterative Threading ASSEmbly Refinement (I-TASSER, https://zhanggroup.org/I-TASSER/) and presented by RasMol Version 2.7.5. The Clustal Omega Multiple

Table 1 Designations and nucleotide sequences of the primers were used in this study

Primer	Sequence (5′-3′)
oligo (Dt)	TTTTTTTTTTTTTTT
SbCTL-F	ATGCTTTATTTTTTGTTCCTAGTG
SbCTL-R	CTAAAGACGTACCGGTCTCTCAC
BF	GTCGCATCTTTGGATTTAACAA
B4	ACTGGGATCCGACTGACAAC
BP	FAM-TGCCCCTGTCATCTTGAGGTATAGACAATC-BHQ
T7	TAATACGACTCACTATAGGG
T7-terminator	TGCTAGTTATTGCTCAGCGG
RT-EF-F	AGTCACCAAGGCTGCACAGAAAG
RT-EF-R	TCCGACGTATTTCTTTGCGATGT
SbCTL-F-C2	CTCTTTACCATGAAGATACCCACC
SbCTL-R-C6	GTGCACGGCTTACCATTTTT
SbCTL-BamH Ⅰ-F	CGCGGATCCGCTTTATTTTTTGTTCCTAGTG
SbCTL-Not Ⅰ-R	AAGGAAAAAAGCGGCCGCAAAGACGTACCGGTCTCTCAC
TF	GGCGTAAAGCGCATGCAGGT
TR	GAAATTCTACCCCCCTCTACAG
VF	CGCCAGGGTTTCCCAGTCACGAC
VR	CACACAGGAAACAGCTATGAC

Alignment program (http://www.ebi.ac.uk/clustalox/) was used to perform the multiple sequence alignment. An unrooted phylogenetic tree of various CTLs containing single CRD was constructed based on the sequence alignment by the neighbor-joining (NJ) algorithm using the Mega 5.0 program (Song *et al.*, 2019). To derive confidence values for the phylogenetic analysis, the Bootstrap test was repeated 1000 times.

The expression and purification of recombinant SbCTL protein

Recombinant SbCTL (rSbCTL) were expressed with pET-30a system (Novagen). The coding region of SbCTL was amplified by the primers SbCTL-BamHI-F and SbCTL-NotI-R, BamHI and NotI endonuclease digestion sites were added at their 5' end, respectively (Table 1). The PCR products were digested with BamHI and NotI endonucleases, gel-purified, then ligased to linearized pET-30a that was digested and recycled in the same way, the recombined expression vector pET-30a-SbCTL was verified by DNA sequencing. Finally, the recombined pET-30a-SbCTL was transformed into Transetta (DE) (TransGen Biotech).

The positive colony was incubated and induced by 1 mM isopropyl-β-d- thiogalactoside (IPTG). Then rSbCTL was purified by a Ni^{2+} chelating Sepharose column, eluted by 500 mM imidazole under denatured condition (8 M urea). The purified proteins were re-natured in gradient urea-TBS glycerol buffer (50 mM Tris-HCl, 50 mM NaCl, 15 % glycerol, 2 mM reduced glutathione, 0.2 mM oxide glutathione, a gradient urea concentration of 6, 4, 3, 2, 1, 0 mM, pH 7.6; dialyzed under each gradient at 4 °C for 12 h). Protein concentration was determined by BCA method (Walker, 1994).

PAMPs binding assay

The PAMPs-binding activity of rSbCTL was assessed by enzyme-linked immune sorbent assay (ELISA) according to previous report with modification. Briefly, 100 μg of LPS, PGN, Man and CpG diluted in 100 μL carbonate-bicarbonate buffer (35 mmol L^{-1} $NaHCO_3$, 15 mmol L^{-1} Na_2CO_3, pH 9.6) were used to coat a 96-well plate. The wells were blocked with 5 % BSA (Sangon Biotech, China) in TBST at 37 °C for 1 h, and then washed with TBST for three times. 100 μL of gradient diluted rSbCTL (containing 0 mM, 10 mM and 100 mM $CaCL_2$) was added sequentially to the wells and incubated for 1 h at 37 °C. The same concentration of rTrx was used as negative control. After three times washing with PBST and then the bound protein was detected immunochemically. Firstly, 100 μL of HRP-labeled goat-anti-HRP-conjugated mouse anti-His-Tag mAb (Sangon Biotech, China, diluted 1:2000 in 5 % BSA) was added into each well and incubated at 37 °C for

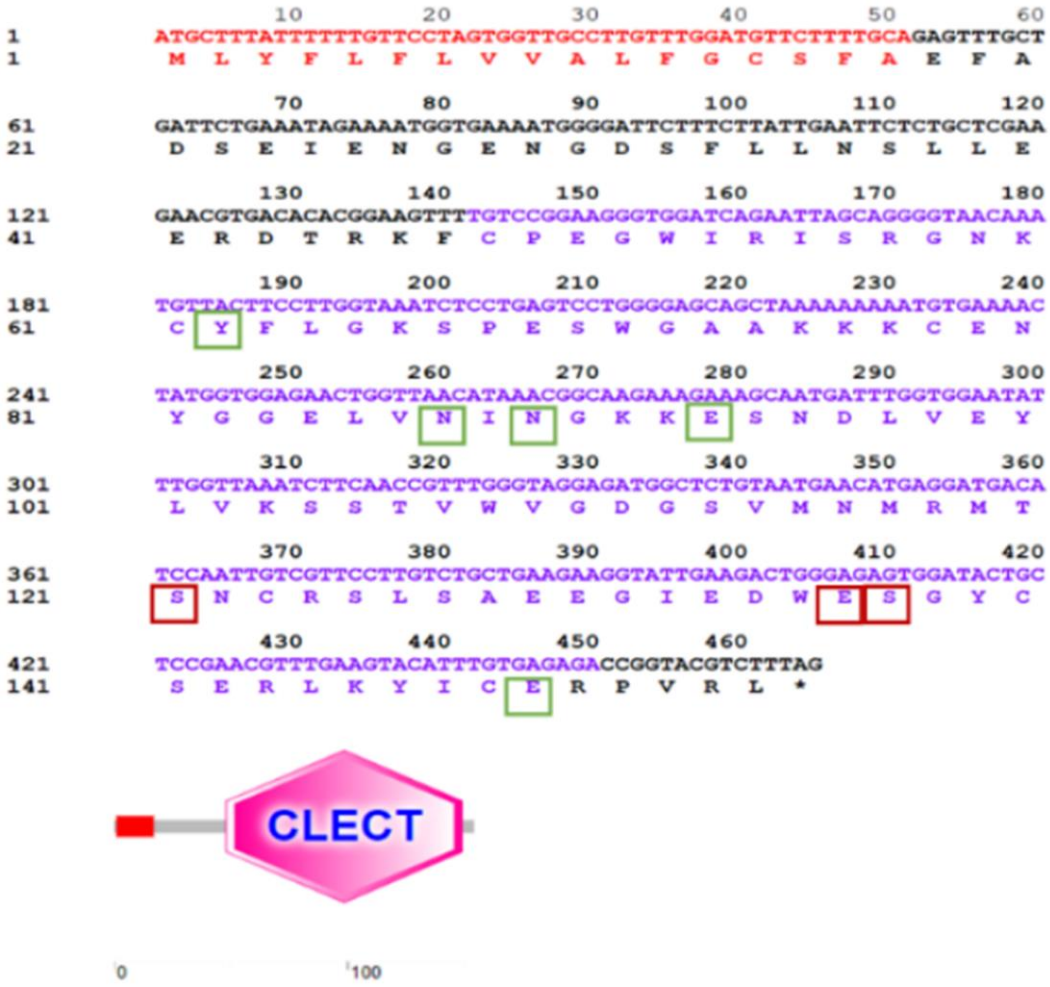

Fig. 1 Nucleotides and deduced amino acid sequences of SbCTL. Nucleotides and amino acids are labelled with numbers on the left of each line, with the green and red boxes representing the two predicted Ca^{2+} binding sites, respectively. The functional domains predicted by the SMART program are marked with different colours: red for signal peptides and dark pink for CRD

1 h. After another three times washing, 100 µL TMB single component substrate solution (Solarbio, Beijing) was added and incubated at 37 °C for 15 min. The reaction was stopped by adding 50 µL of 2 M termination solution per well, and the absorbance was measured at 405 nm (TECAN, Switzerland). The wells with 100 µL TBS were used as blank. The non-immunized mouse serum was employed as negative control. Three replications were performed for each sample, and the data were presented as mean ± S.D. (n = 3). Samples with P (sample)-B (blank)/N (negative) - B (blank) > 2.1 were considered as positive.

Quantification of OsHV-1

The samples of hemocytes were collected at 0 h, 24 h, 48 h and 72 h post the injection of OsHV-1 in ark clams. Tissue genomic DNA was extracted using the DNeasy Blood and Tissue kit (Qiagen) following the manufacturer's instructions. DNA concentration and quality were assessed by spectrophotometer (NanoDrop2000, Thermo-Scientific). To reduce individual differences, each DNA sample was prepared from three individuals. Then DNA samples were taken for real-time quantitative PCR (qRT-PCR) with the pair of primers BF/B4 (Table 1) and the probe BP. The reaction system was 20 µL and amplification was performed using CFX Connect from Bio-Rad, USA under the following condition: 1 cycle 95 °C for 10 min, followed by 40 cycles of 95 °C for 10 s, 60 °C for 30 s (Segarra *et al.*, 2010). The OsHV-1 quantitation was calculated from the standard curve, which was created from a 10-fold dilution series (10^7-10^1 copies μL^{-1}) of plasmid containing the target sequence.

Quantification of total Vibrio DNA by qPCR

The qPCR assay based on SYBR® Green described by Julien (De Lorgeril *et al.*, 2018) was used to quantify total vibrio with modification. Tissue samples and DNA extraction were processed as quantification of OsHV-1, differently, each tissue

sample was mixed with equal *Escherichia coli* (10 µL, OD_{600} 1.0) containing plasmid pUC18 as the reference. The primer pairs TF and TR (Table 1) targeting 16S rDNA were designed to relatively quantify Vibrio content by the $2^{-\Delta\Delta Cq}$ method with the measured threshold cycle values of the reference genes in *E. coli* using the primer pairs VF and VR (Table 1). Real-time PCR amplification was carried out in an ABI 7500 Real-time thermal cycler according to the manual (Eppendorf, Hamburg, Germany).

Quantitative real-time PCR analyses of SbCTL *mRNA expression*

SbCTL mRNA expression level was measured by SYBR® green fluorescent quantitative real-time PCR. Two specific primers of SbCTL, SbCTL-F-C2 and SbCTL-R-C6 (Table 1), were designed for RT-PCR amplification. A pair of primers for elongation factor, RT-EF-F and RT-EF-R (Table 1), were chosen for PCR amplification as an internal control. Real-time PCR amplification was carried out in an ABI 7500 Real-time thermal cycler according to the manual (Eppendorf, Hamburg, Germany). Dissociation curve analysis of amplification products was performed at the end of each PCR to confirm the specificity. After the PCR program, the $2^{-\Delta\Delta Cq}$ method was used to analyze the expression level of SbCTL.

Survival rate of S. broughtonii

Ark clams were divided into two groups (with 100 ark clams in each group). One group was injected with 1 µg/µL SbCTL (100 µL), and the other group with the same volume of sterile sea water as control. After 1 h, 100 µL of OsHV-1 inoculum was injected into each ark clams of both groups. The number of surviving ark clams in each group was counted every 12 h post OsHV-1 infection. The survival rate was equal to (surviving ark clams/100) × 100 %. Survival curves were generated by GraphPad Prism 8.0.

Statistical analysis

Data was analyzed using Origin 8.1 (Origin Lab) and Statistical Package for Social Sciences (SPSS) 23.0. Significant differences for each assay were tested by one-way analysis of variance (ANOVA). If significant differences were indicated at the 0.05 level, then a post hoc multiple-comparisons (Tukey's) test was used to examine significant differences among treatments using SPSS. Difference was considered significant at $p < 0.05$ and extremely significant at $p < 0.01$

Results

cDNA clone and sequence analyses of SbCTL

A coding sequence of 465 bp was amplified with specific primers SbCTL-F and SbCTL-R (Table 1). It encoded a polypeptide of 154 amino acids (predicted molecular mass of 17.453 kDa and PI was 4.64). The red colour region showed the signal peptide (position 1st to 17th amino acid). The purple region showed the single carbohydrate recognition structural domain (CRD) of SbCTL with 102 amino acid residues. The CRD of SbCTL has two calcium binding sites, one Ca^{2+} binding site linked to TYR62, ASN87, ASN89, GLU93, GLU149 and the other to SER121, GLU136, SER137 (Fig. 1).

Multiple sequence alignment and phylogenetic analysis of SbCTL

BLAST homology analysis showed that SbCTL has 28 % - 39 % homology with CTLs from the following species (Fig. 2): *Eudyptes pachyrhynchus*

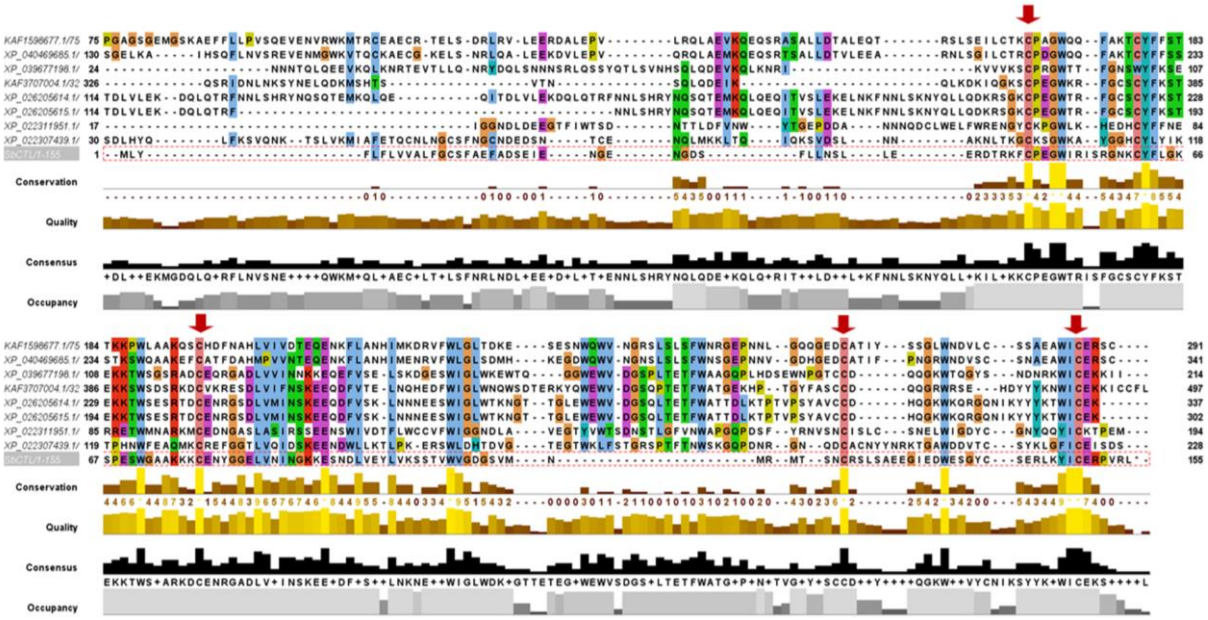

Fig. 2 Multiple sequence alignment of SbCTL with other CTLs, including *Eudyptes pachyrhynchus* (KAF1598677.1); *Channa argus* (KAF3707004.1); *Perca fluviatilis* (XP_039677198.1); *Anabas testudineus* (XP_026205614.1); *A. testudineus* (XP_026205615.1); *A. testudineus* (XP_033181795.1)*; Falco naumanni* (XP_040469685.1)*; Crassostrea virginica* (XP_022311951.1)*; C. virginica* (XP_022307439.1). Red arrows indicate four conserved *cysteine* sites

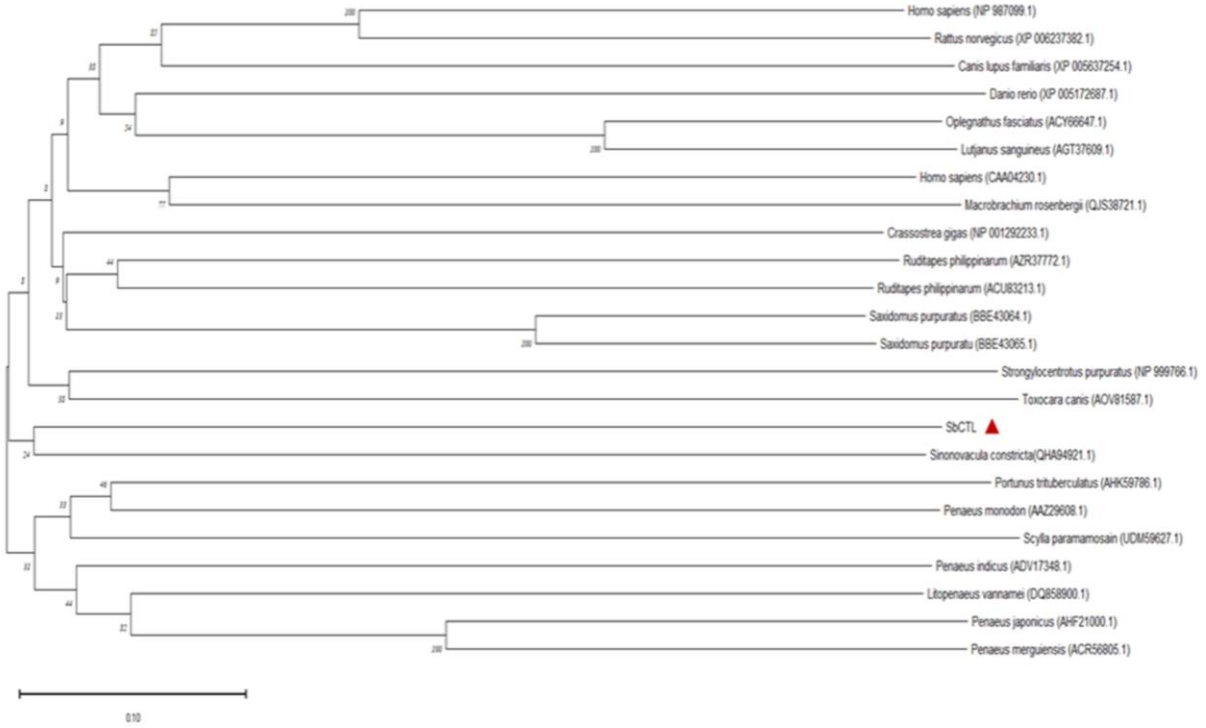

Fig. 3 Phylogenetic tree of CTLs containing a single CRD. Mega 5.0 program was used to construct the tree by Neighbor-joining (NJ) algorithm based on the multiple sequence alignment. The optimal tree is shown. The reliability of the branching was tested by bootstrap re-sampling (1000 pseudo-replicates). The CTLs used in phylogenetic tree were listed as the following: *Homo sapiens (NP_987099.1)*；*Homo sapiens (CAA04230.1); Crassostrea gigas (NP_001292233.1); Strongylocentrotus purpuratus (NP_999766.1); Canis lupus familiaris (XP_005637254.1); Danio rerio (XP_005172687.1); Litopenaeus vannamei (DQ858900.1); Penaeus indicus (ADV17348.1); Portunus trituberculatus (AHK59786.1); Oplegnathus fasciatus (ACY66647.1); Lutjanus sanguineus (AGT37609.1); Penaeus monodon (AAZ29608.1); Rattus norvegicus (XP_006237382.1); Ruditapes philippinarum (AZR37772.1); Macrobrachium rosenbergii (QJS38721.1); Scylla paramamosain (UDM59627.1); Toxocara canis (AOV81587.1); Sinonovacula constricta (QHA94921.1); Saxidomus purpuratus (BBE43064.1); Saxidomus purpuratu (BBE43065.1); Penaeus japonicus (AHF21000.1); Ruditapes philippinarum (ACU83213.1); Penaeus merguiensis (ACR56805.1)*

(KAF1598677.1); *Channa argus* (KAF3707004.1); *Perca fluviatilis* (XP_039677198.1); *Anabas testudineus* (XP_026205614.1); *A. testudineus* (XP_026205615.1); *A. testudineus* (XP_033181795.1); *Falco naumanni* (XP_040469685.1); *Crassostrea virginica* (XP_022311951.1)*; C. virginica* (XP_022307439.1). The highest similarity was found with *A. testudineus* at 39.19%. Similarity with *C. argus* was higher at 37.5%. Four cysteines (Cys48; Cys78; Cys120; Cys148) were conservatively existed in all selected CTLs as the red arrow shown, these four conserved cysteine residues are involved in the formation of disulfide bonds within the CRD.

To evaluate the molecular evolutionary relationships between SbCTL and other CTLs containing a single CRD, a phylogenetic tree was constructed using the NJ algorithm (1000 bootstrap replicates) based on the amino acid sequences of 18 CTLs (Fig. 3). Of the selected species, *Homo sapiens*, *Canis lupus familiaris* and *Rattus norvegicus* belong to the *Chordata* phylum *Mammalia*. *Danio rerio*, *Oplegnathus fasciatus* and *Lutjanus sanguineus* belong to the *Chordata* phylum *Pisce*. *Strongylocentrotus purpuratus* belongs to the *Echinodermata* phylum *Echinoidea*. *C. gigas, Saxidomus purpuratus, Sinonovacula constricta* and *Ruditapes philippinarum* belong to the *Mollusca* phylum *Bivalvia.* In the phylogenetic tree, the SbCTL is clustered in a branch with the CTL of a bivalve species, *S. constricta*, and is most closely related to other bivalve CTLs.

The predicted three-dimensional structure of SbCTL

The potential three-dimensional structure of SbCTL was established by the I-TASSER. The CRD of SbCTL composed of two α-helices and five β-strands forming a bilayer structure. Two potential Ca^{2+} binding sites were shown in CRD. The two Ca^{2+} binding sites are located at TYR3 and GLU129. A MAN binding domain were also indicated with five amino acids (SER127, GLU136, GLY138, THR106, SER125) linked together (Fig. 4).

The purified protein and PAMP-binding specificity of rSbCTL

SDS-PAGE showed a distinct band with a molecular mass of ~25 KD in the lane of purified

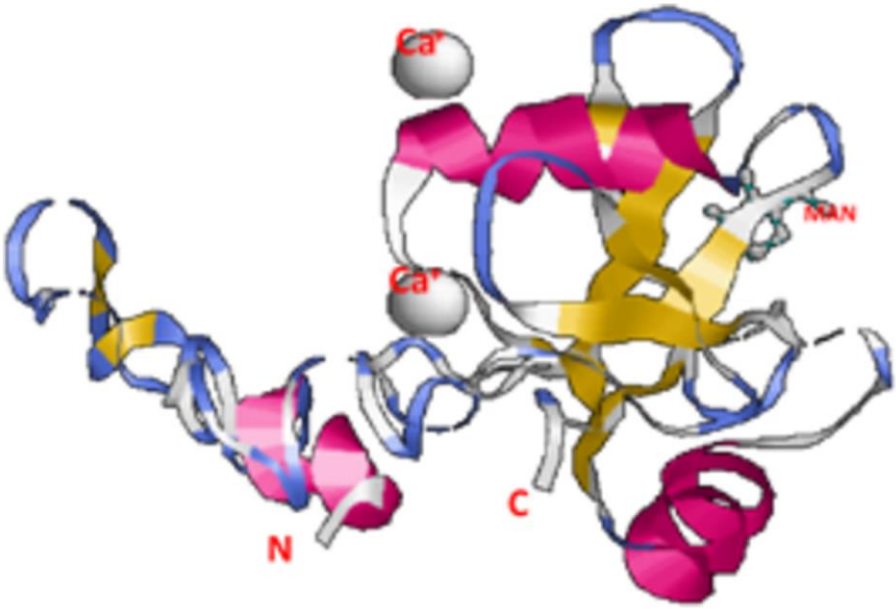

Fig. 4 The I-TASSER program predicts the structure of SbCTL. Random coil marked as white, β-stands marked as yellow and α-helices marked as red. The grey and blue spheres forming the cyclic structural domain are MAN binding sites

rSbCTL, which was consistent with the predicted molecular mass of SbCTL (Fig. 5).

The PAMP-binding capacity of rSbCTL was recorded as P/N at 405 nm, and the samples with P/N > 2.1 were considered as positive. In the presence of Ca^{2+} or not, the P/N values for LPS and MAN were greater than 2.1, with the concentration of 100 μg/Ml to 1.5625 μg/Ml respectively. rSbCTL showed the highest affinity to LPS, lower affinity to MAN, and almost no affinity to PGN and CPG. The P/N values for LPS and MAN showed inapparent change with different Ca^{2+} concentration. (Fig. 6).

The load change of OsHV-1 in infected ark clams

The quantification of OsHV-1 was performed by real-time PCR based on Taqman probe method. The OsHV-1 DNA load in these tissues sharply increased to ~10^7 copies per ng total DNA within 48 h. After that, OsHV-1 copies tended to sustain at this level without ongoing increase (around 10^7 copies/ng total DNA). (Fig. 7).

Total vibrio quantity post OsHV-1 infection

The total vibrio in ark clam hemocytes at 0, 24, 48 and 72 h after OsHV-1 infection (Fig. 8) was further examined. After OsHV-1 stimulation, vibrio content in hemocytes decreased at 24 h, then increased before reaching peak levels at 72 h (4.25-fold that in 0h, $p < 0.05$) at 72 h.

The mRNA expression pattern of SbCTL

The distribution of SbCTL *mRNA* was investigated in tissues, including hemocytes, mantle, foot, gill, hepatopancreas and adductor muscle. The transcripts of SbCTL *mRNA* could be detected in all tested tissues. The highest transcript levels of SbCTL

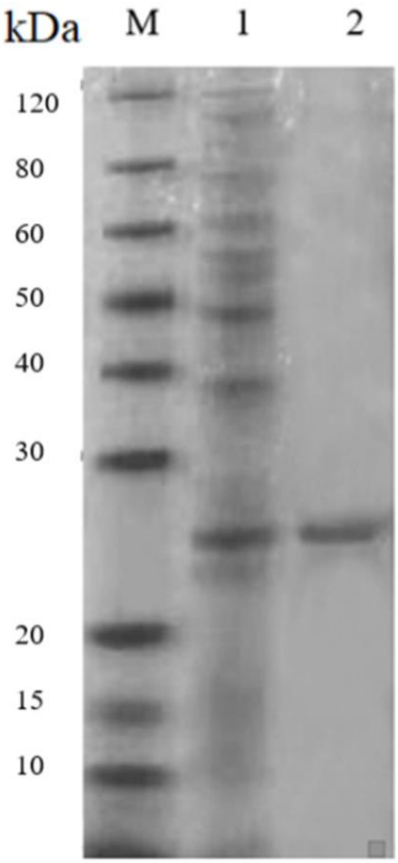

Fig. 5 SDS-PAGE of rSbCTL. Lane M: protein molecular standard; lane 1: lysate of E. coli Transetta cells transformed with Pet-30a with IPTG induction; lane 2: purified rSbCTL protein

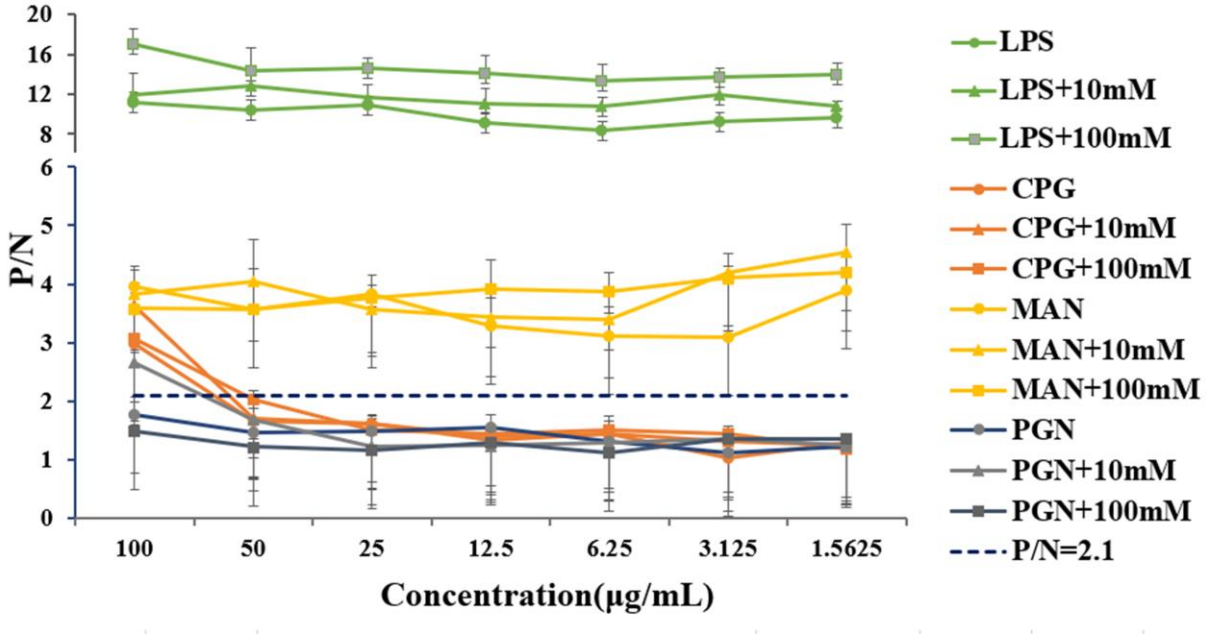

Fig. 6 ELISA analysis of rSbCTL binding activity to PAMPs, including LPS, PGN, MAN and CPG. The value of P/N > 2.1 was considered positive. 10mM and 100mM indicate the concentration of $CaCL_2$. Results represent the mean of three replicates ± S.D.

mRNA were found in the gills ($p < 0.05$), while the lowest in adductor muscle. There were no significant differences of SbCTL mRNA expression in hemocytes, mantle, foot and hepatopancreas ($p > 0.05$). (Fig. 9A).

The *mRNA* expression of SbCTL in response to OsHV-1 infection was analyzed in hemocytes. At the early stage of OsHV-1 infection, OsHV-1 DNA copies increased sharply (Fig. 7), while the level of SbCTL *mRNA* showed inapparent change post 48 h infection ($p > 0.05$). Later OsHV-1 DNA copies reached a plateau (~10^7 copies per ng total DNA), the level of SbCTL *mRNA* increased significantly post 72 h infection compared to the prior time points (Fig. 9B).

The protection role of rSbCTL in vivo

The survival rates of OsHV-1 infected ark clams were recorded in both rSbCTL treated group and control group. The control group was set with the OsHV-1 infection only, and the experimental group was pretreated with rSbCTL prior to OsHV-1 infection. The results showed that the survival rate of the control group began to decline post 48 h infection, while no death was simultaneously found in the rSbCTL treatment group. After 72 h of infection, the survival rate of the rSbCTL treatment group decreased to 85 %, meanwhile the control group decreased to 48.14 %. After 108 h infection, the survival rate of the experimental group was 30 % and that of the control group was only 5.55 %. Survival curve comparation of both groups showed significant difference ($p < 0.05$) using the method of Log-rank (Mantel-Cox) test. (Fig. 10)

Discussion

CTLs, as members of the PRRs, are crucial in the initial non-self recognition by the binding between their CRDs and specific carbohydrate structures on the surface of microorganisms. A single and multiple CRDs-containing CTLs conservatively exist in invertebrates, recognize various PAMPs and activate intracellular immune

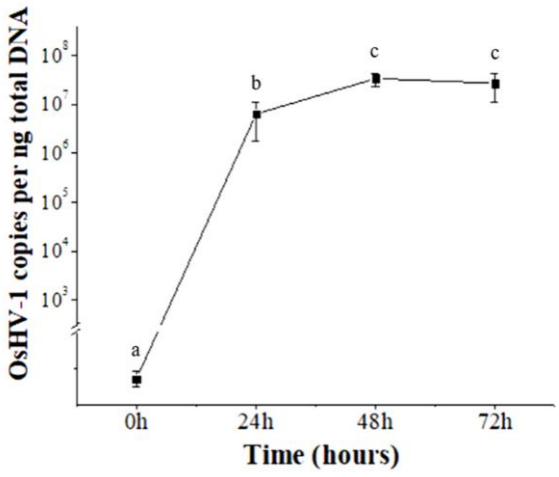

Fig. 7 The load changes of OsHV-1 at different time points in the hemocytes of ark clams. OsHV-1 load was expressed as the OsHV-1 copies in per ng total tissue DNA. Each value was shown as mean ± S.D. (N = 3)

signal pathways against pathogens (Wang *et al.*, 2007; Zhang *et al.*, 2009b; Kong *et al.*, 2011). In contrast to vertebrate CTLs, the immunological function of invertebrate CTLs defects in comprehensive understanding. In this study, a new member of the CTLs containing a single CRD, SbCTL, was identified from ark clams, *S. broughtonii*. The sequence characteristics and biological activities of SbCTL were investigated in order to gain more understanding of their role in ark clam innate immunity.

SbCTL was highly conserved in sequential and structural features with other CTLs. A signal peptide at the N-terminal end of SbCTL revealed that SbCTL could function as a secreted CTL. Four cysteine residues involved in the formation of the internal disulfide bridges were well conserved in the CRD of SbCTL. According to available studies, there were commonly four Ca^{2+} binding sites in CRDs of CTLs. The recognition activity and binding specificity of CTLs depends on the location of the proton donor and proton acceptor at Ca^{2+} binding site (Zelensky and Gready, 2005). Two Ca^{2+}-binding site was also predicted in the CRD of SbCTL, suggesting Ca^{2+} might be needed for SbCTL binding to carbohydrates. However, Ca^{2+} binding site is not necessary for all CTLs, such as two CTLs, SPL-1 and SPL-2, that were capable of binding to acetamide-containing carbohydrates in the absence of Ca^{2+} in *S. purpuratus* (Unno *et al*., 2019; Unno *et al*., 2020).

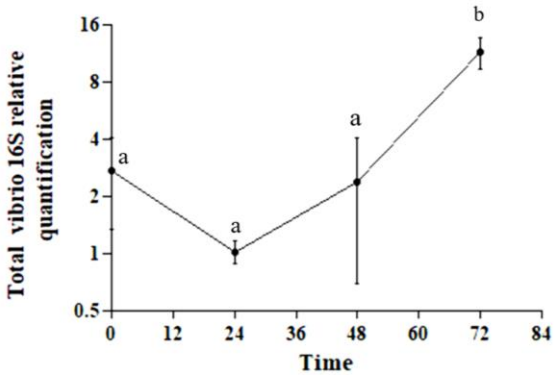

Fig. 8 The change of total vibrio post OsHV-1 infection. The total vibrio in ark clam hemocytes after OsHV-1 infection was detected by real-time PCR at 0, 24, 48 and 72 h. Each value was shown as mean± S.D. (N=3). The significant difference among groups is indicated by dissimilar letters ($p < 0.05$)

The recognition and binding to PAMPs is one of the most important properties of CTLs, which was achieved by the CRDs of CTLs. Multiple-CRDs containing CTLs possess broader recognition spectrum than CTLs containing a single CRD. Conversely, a single CRD containing CTLs are

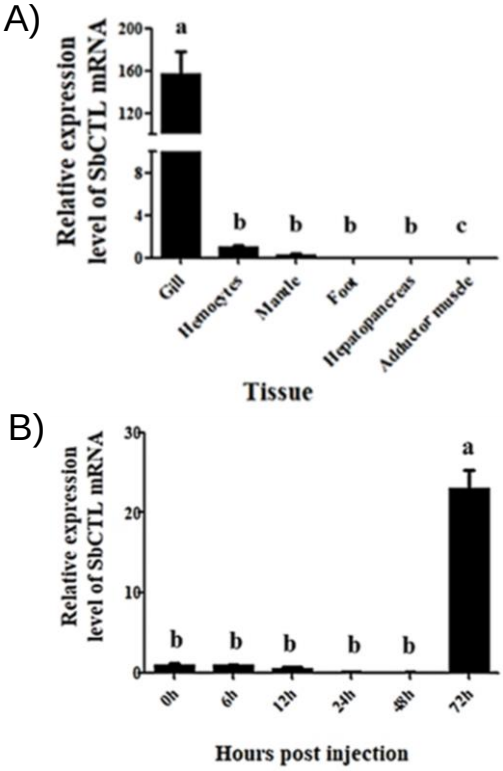

Fig. 9 Real-time PCR analyses of SbCTL. A) SbCTL mRNA expression levels in different tissues of ark clam *S.broughtonii*. SbCTL mRNA expression levels in mantle, gills, hemocytes, foot, muscle and hepatopancreas were all normalized to that of muscle. Vertical bars represent the mean ± S.D. (N = 6). The significant difference among groups is indicated by dissimilar letters ($p < 0.05$). B) At 0, 6, 12, 24, 48 and 72 h after OsHV-1 challenge, hemocytes were collected and the mRNA transcription patterns of SbCTL were detected by real-time PCR. The cytb gene was used as an internal control to calibrate the cDNA template for all the samples. Each value was shown as mean ± S.D. (N = 3). The significant difference among groups is indicated by dissimilar letters ($p < 0.05$)

relatively more specific. SbCTL contains a single CRD, showed dissimilar binding activity to various PAMPs. SbCTL performed the strongest binding activity to LPS, lower to MAN, and almost none to PGN and CPG, implying that SbCTL might focus on the recognition of bacteria. Ca^{2+} binding site seems not necessary for the binding activity of SbCTL to PAMPs, though there were two Ca^{2+} binding sites predicted in SbCTL. Even without Ca^{2+}, SbCTL also showed high binding activity to LPS and MAN.

Death of bivalves caused by OsHV-1 infection went through two stages. During primary OsHV-1 infection, viral rapid replication leads to the host entering an immune-compromised state. Then opportunistic bacteria were liable to invade the OsHV-1 infected bivalves, which constituted secondary bacterial infection (de Lorgeril *et al.*, 2018). In healthy ark clams, there were constitutive expression of SbCTL in tissues. During primary OsHV-1 infection, OsHV-1 DNA copies increased sharply, SbCTL might not sense nor directly binding to OsHV-1, it showed extremely low binding activity to nucleic acid PAMPs. SbCTL was not mobilized during the primary OsHV-1 infection, the mRNA expression of SbCTL kept stable until the next stage. After infection with OsHV-1, the vibrio content in ark clam reached a peak at 72 h (Fig. 8). This phenomenon was consisted with the expression pattern of SbCTL (Fig. 9b) in hemocytes post OsHV-1 infection. Thus, it was speculated that the delayed up-regulation of SbCTL mRNA might contribute to protect hosts from secondary bacteria infection (Fig. 11).

In summary, a C-type lectin (SbCTL) with a signal peptide and a CRD structure was identified from *S. broughtonii*. SbCTL showed especially high binding activity to LPS in a Ca^{2+}-independent manner. SbCTL constitutively expressed in tissues and could respond to OsHV-1 infection at the late stage. rSbCTL pretreatment *in vivo* showed a significant protection effect against OsHV-1 infection.

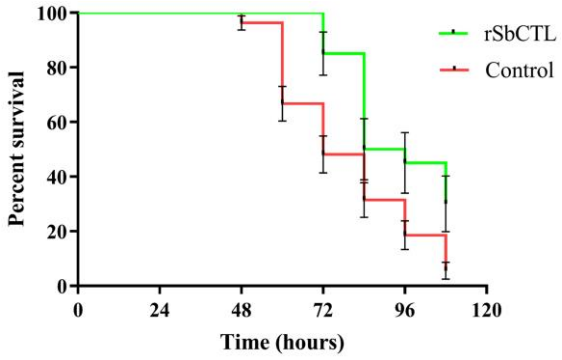

Fig. 10 Survival rate of ark clams after OsHV-1 infection. rSbCTL presents the group with rSbCTL treated *in vivo*, Control presents the group treated with the same volume of filtered seawater. The number of survival individuals were recorded at 24, 46, 60, 72, 84, 96 and 108 h, respectively

To sum up, we presumed that SbCTL served a protection role in the innate immunity of *S. broughtonii* by recognizing and binding to PAMPs of intruders.

Acknowledgements

We are grateful to all the laboratory members for their technical support and helpful comments. This research was financially supported by the National Natural Science Foundation of China (Grant number: U1706204, 31902400), the Special Scientific Research Funds for Central Non-profit Institutes, Yellow Sea Fisheries Research Institutes (Project No. 20603022020007 and 20603022021012), Key Laboratory of Healthy Mariculture for the East China Sea (Grant number: 2020ESHML08), China Agriculture Research System of MOF and MARA.

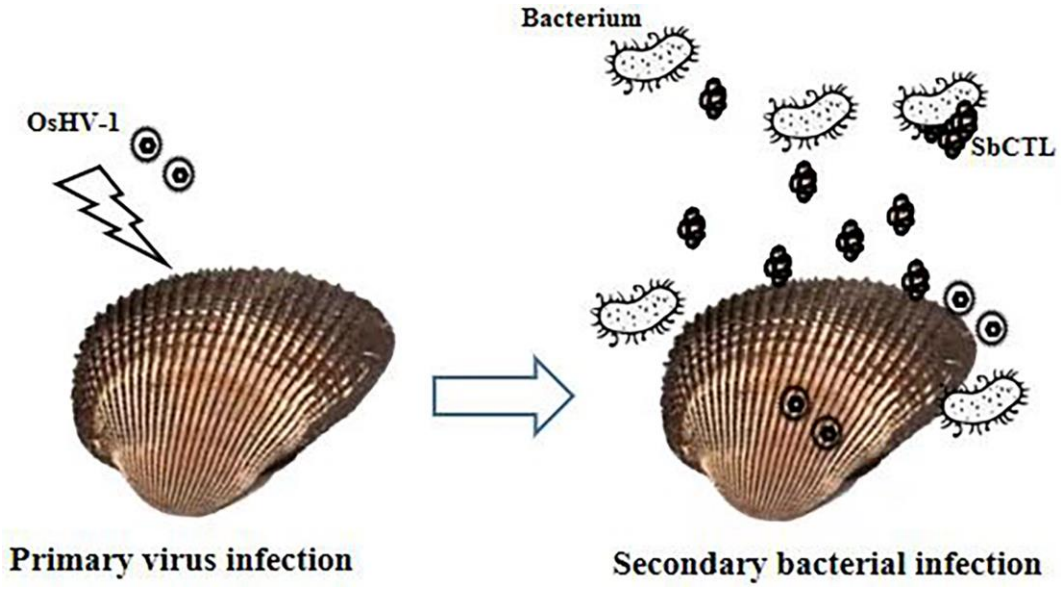

Fig. 11 The deduced functional process of SbCTL in ark clams post OsHV-1 infection

References

De Lorgeril J, Aude L, Bruno P, Toulza E, Montagnani C, Clerissi C, *et al*. Immune-suppression by OsHV-1 viral infection causes fatal bacteraemia in Pacific oysters. Nat Commun. 9, 2018.

Eisen DP. Mannose-Binding Lectin Deficiency and Respiratory Tract Infection. J Innate Immun. 2: 114-122, 2010.

Junkunlo K, Anuphap P, Amornrat T, Senapin S, Borwornpinyo S, Flegel TW, *et al*. A novel lectin domain-containing protein (LvCTLD) associated with response of the whiteleg shrimp *Penaeus* (*Litopenaeus*) *vannamei* to yellow head virus (YHV). Dev Comp Immunol. 37: 334-341, 2012.

Kong P, Wang L, Zhang H, Song X, Zhou Z, Yang J, *et al*. A novel C-type lectin from bay scallop *Argopecten irradians* (AiCTL-7) agglutinating fungi with mannose specificity. Fish Shellfish Immunol. 30: 836-844, 2011.

Luo T, Fang L, Lei K, Xu X. Genomic organization, promoter characterization and expression profiles of an antiviral gene PmAV from the shrimp *Penaeus monodon*. Mol Immunology. 44: 1516-1523, 2007.

Ren Q, Zhou J, Jia YP, Wang XW, Zhao XF, Wang JX. Cloning and characterization of Rap GTPase from the Chinese white shrimp *Fenneropenaeus chinensis*. Dev Comparative Immunol. 36, 2012.

Ren W, Chen H, Renault T, Cai Y, Bai C, Chongming Wang C, *et al*. Complete genome sequence of acute viral necrosis virus associated with massive mortality outbreaks in the Chinese scallop, *Chlamys farreri*. Virol J. 10, 2013.

Segarra A, Pepin JF, Arzul I. Detection and description of a particular Ostreid herpesvirus 1 genotype associated with massive mortality outbreaks of Pacific oysters, *Crassostrea gigas*, in France in 2008. Virus Res. 153: 92-99, 2010.

Shi L, Takahashi K, Dundee J, Sarit SK, Thiel S, Jensenius JC, *et al*. Mannose-binding lectin-deficient mice are susceptible to infection with *Staphylococcus aureus*. J Exp Med. 199: 1379-1390, 2004.

Song X, Xin X, Wang H, Li H, Zhang H, Jia Z, *et al*. A single-CRD C-type lectin (CgCLec-3) with novel DIN motif exhibits versatile immune functions in *Crassostrea gigas*. Fish Shellfish Immunol. 92: 772-781, 2019.

Sorvillo N, van Haren SD, Pos W, Herczenik E, Fijnheer R, Martinez-Pomares L, *et al*. C-Type Lectin Receptor Mediated Immune Recognition of ADAMTS13 Promotes HLA-DRB1*11 Dependent Presentation of CUB1-2 Derived Peptides by Dendritic Cells. Blood. 118: 92-93, 2011.

Unno H, Higuchi S, Goda S, Hatakeyama T. Novel carbohydrate-recognition mode of the invertebrate C-type lectin SPL-1 from *Saxidomus purpuratus* revealed by the GlcNAc-complex crystal in the presence of Ca^{2+}. Acta Crystallogr F Struct Biol Commun. 76: 271-277, 2020.

Unno H, Itakura S, Higuchi S, Goda S, Kenichi Yamaguchi K, Hatakeyama T. Novel Ca^{2+}-independent carbohydrate recognition of the C-type lectins, SPL-1 and SPL-2, from the bivalve *Saxidomus purpuratus*. Protein Sci. 28: 766-778, 2019.

Vasta GR, Ahmed H, Odom EW. Structural and functional diversity of lectin repertoires in invertebrates, protochordates and ectothermic vertebrates. Curr Opin Struct Biol. 14: 617-630, 2004.

Vezzulli L, Brettar I, Pezzati E, Reid PC, Colwell RR, Hofle MG, *et al*. Long-term effects of ocean warming on the prokaryotic community: evidence from the vibrios. ISME J. 6: 21-30, 2012.

Walker JM. The bicinchoninic acid (BCA) assay for protein quantitation. Methods Mol Biol. 32, 1994.

Wang H, Song L, Li C, Zhao J, Zhang H, Ni D, *et al*. Cloning and characterization of a novel C-type lectin from Zhikong scallop *Chlamys farreri*. Mol Immunol. 44: 722-731, 2007.

Wang L, Wang L, Jiang Y, Zhang H, Huang M, Kong P, *et al*. A multi-CRD C-type lectin with broad recognition spectrum and cellular adhesion from Argopecten irradians. Dev Comp Immunol. 36: 591-601, 2012.

Wang J, Wang L, Yang C, Jiang Q, Zhang H, Yue F, *et al*. The response of mRNA expression upon secondary challenge with Vibrio anguillarum suggests the involvement of C-lectins in the immune priming of scallop *Chlamys farreri*. Dev Comp Immunol. 40: 142-147, 2013.

Watanabe A, Miyazawa S, Kitami M, Tabunoki H, Ueda K, Sato R. Characterization of a novel C-type lectin, *Bombyx mori* multi-binding protein, from the B-mori hemolymph: Mechanism of wide-range microorganism recognition and role in immunity. J Immunol. 177: 4594-4604, 2006.

Wu T, Shi X, Zhou Z, Wang L, Wang M, Wang L, *et al*. An iodothyronine deiodinase from *Chlamys farreri* and its induced mRNA expression after LPS stimulation. Fish Shellfish Immunol. 33: 286-293, 2012.

Zelensky AN, Gready JE. The C-type lectin-like domain superfamily. FEBS J. 272: 6179-6217, 2005.

Zhang H, Wang H, Wang L. A novel C-type lectin (Cflec-3) from *Chlamys farreri* with three carbohydrate-recognition domains. Fish Shellfish Immunol. 26: 707-715, 2009a.

Zhang XW, Xu WT, Wang XW, Mua Y, Zhao XF, Yu XQ, *et al*. A novel C-type lectin with two CRD domains from Chinese shrimp *Fenneropenaeus chinensis* functions as a pattern recognition protein. Mol Immunol. 46: 1626-1637, 2009b.

Zhang XW, Man X, Huang X, Wong Y, Song QS, Hui KM, *et al*. Identification of a C-type lectin possessing both antibacterial and antiviral activities from red swamp crayfish. Fish Shellfish Immunol. 77: 22-30, 2018.

Zhao Q, Wu B, Liu Z, Sun X, Zhou L, Yang A, *et al*. Molecular cloning, expression and biochemical characterization of hemoglobin gene from ark shell *Scapharca broughtonii*. Fish Shellfish Immunol. 78, 2018.